2

AL/OE-TR-1995-0122

ARMSTRONG LABORATORY

THEORETICAL STUDIES ON SHORT-PULSE OCULAR DAMAGE

Lihong Wang

TASC
750 East Mulberry, Suite 302
San Antonio, Texas 78212

OCCUPATIONAL AND ENVIRONMENTAL HEALTH DIRECTORATE
Optical Radiation Division
8111 18th Street
Brooks Air Force Base, Texas 78235-5215

August 1995

Interim Report for Period March 1994 - August 1994

Approved for public release; distribution is unlimited.

AIR FORCE MATERIEL COMMAND
BROOKS AIR FORCE BASE, TEXAS

NOTICES

When Government drawings, specifications, or other data are used for any purpose other than in connection with a definitely Government-related procurement, the United States Government incurs no responsibility or any obligation whatsoever. The fact that the Government may have formulated or in any way supplied the said drawings, specifications, or other data, is not to be regarded by implication, or otherwise in any manner construed, as licensing the holder or any other person or corporation; or as conveying any rights or permission to manufacture, use, or sell any patented invention that may in any way be related thereto.

The mention of trade names or commercial products in this publication is for illustration purposes and does not constitute endorsement or recommendation for use by the United Sates Air Force.

The Office of Public Affairs has reviewed this report, and it is releasable to the National Technical Information Service, where it will be available to the general public, including foreign nationals.

This report has been reviewed and is approved for publication.

Government agencies and their contractors registered with Defense Technical Information Center (DTIC) should direct requests for copies to: DTIC, Building 5, Cameron Station, 5010 Duke Street, Alexandria VA 22304-6145.

Non-government agencies may purchase copies of this report from: National Technical Information Service (NTIS), 5285 Port Royal Road, Springfield VA 22161-2103.

Robert M Cartledge

ROBERT M. CARTLEDGE, Lt Col, USAF, BSC
Chief, Optical Radiation Division

REPORT DOCUMENTATION PAGE

Form Approved
OMB No. 0704-0188

1. AGENCY USE ONLY (Leave blank)	2. REPORT DATE	3. REPORT TYPE AND DATES COVERED
	August 1995	Interim - March 1994 - August 1994

4. TITLE AND SUBTITLE

Theoretical Studies on Short-Pulse Ocular Damage

5. FUNDING NUMBERS

C - F33615-92-C-0017
PE - 62202F
PR - 2312
TA - A1
WU - 01

6. AUTHOR(S)

Lihong Wang

7. PERFORMING ORGANIZATION NAME(S) AND ADDRESS(ES)

TASC
750 East Mulberry
Suite 302
San Antonio, TX 78212-3159

8. PERFORMING ORGANIZATION REPORT NUMBER

9. SPONSORING/MONITORING AGENCY NAME(S) AND ADDRESS(ES)

Armstrong Laboratory
Occupational and Environmental Health Directorate
Optical Radiation Division
8111 18th Street
Brooks Air Force Base, TX 78235-5215

10. SPONSORING/MONITORING AGENCY REPORT NUMBER

AL/OE-TR-1995-0122

11. SUPPLEMENTARY NOTES

12a. DISTRIBUTION/AVAILABILITY STATEMENT

Approved for public release; distribution is unlimited.

12b. DISTRIBUTION CODE

13. ABSTRACT *(Maximum 200 words)*

A theoretical analysis has been performed for the phase transitions from liquid to gas on the boundary of a spherical particle, submerged in a fluid such as water or ocular media, that is heated by absorption of sub-nanosecond laser pulses. This analysis was based on the conservation of mass and it utilized the general heat conduction equation for the principle of conservation of energy and the basic hydrodynamic equation for the incompressible fluid for the expression of conservation of momentum. The research results of underwater explosions were reviewed and the motion of underwater explosion bubbles was analyzed for relevance to the production of bubbles produced by both the short- and long-pulsewidth lasers. Also, bubble motion was analyzed in terms of compressive and noncompressive surrounding medium. Finally, analytical expressions were derived for the maximum bubble radius as a function of input energy and the bubble oscillation period as a function of both input energy and ambient pressure.

14. SUBJECT TERMS

Bubble; Hydrodynamic equation; Motion; Ocular media

15. NUMBER OF PAGES

16. PRICE CODE

17. SECURITY CLASSIFICATION OF REPORT	18. SECURITY CLASSIFICATION OF THIS PAGE	19. SECURITY CLASSIFICATION OF ABSTRACT	20. LIMITATION OF ABSTRACT
Unclassified	Unclassified	Unclassified	UL

TABLE OF CONTENTS

FIGURES

Figure No. **Page**

THEORETICAL STUDIES ON SHORT-PULSE OCULAR DAMAGE

PROBLEM

The theoretical study reported is part of a larger, more comprehensive project. This simplified model illustrates that a short-pulse laser beam is incident on water containing a melanin granule. The water is considered transparent, and the melanin granule is highly absorbing. After the delivery of the laser beam, an acoustic wave (maybe a shock wave) is established around the granule and propagates in the water. Bubbles may be formed around the melanin granule. The goal is to compute the amplitude and propagation of the shock wave and the bubble motion so that tissue damage can be estimated. Alternatively, the threshold energy density causing minimal visible lesions (MVLs) can be estimated based on the damage threshold of tissues. This project will concentrate on the formation, growth, and collapse of bubbles although the author will express his opinions and study results on related issues.

TERMINOLOGY

The problem involves more than one phase. A simple classification is shown in Figure 1. In our specific problem, the water is the continuous phase, and the melanin granule is considered the dispersed phase (solid particle). The bubble caused by the laser absorption will belong to the dispersed phase.

When a body of liquid is heated under constant pressure, or when its pressure is reduced at constant temperature by static or dynamic means, a state is reached ultimately at which vapor or gas- and vapor-filled bubbles, or cavities, become visible and grow. The bubble growth may be at a nominal rate if it is caused by the diffusion of dissolved gases into the cavity or merely by expansion of the gas content with temperature rise or pressure reduction. The bubble growth will be "explosive" if it is primarily the result of vaporization into the cavity. This condition is known as boiling if caused by temperature rise, and cavitation if caused by dynamic-pressure reduction at essentially constant temperature. Bubble growth by diffusion is termed degassing although it is also called gaseous cavitation (in contrast to vaporous cavitation) when induced by dynamic-pressure reduction.[1]

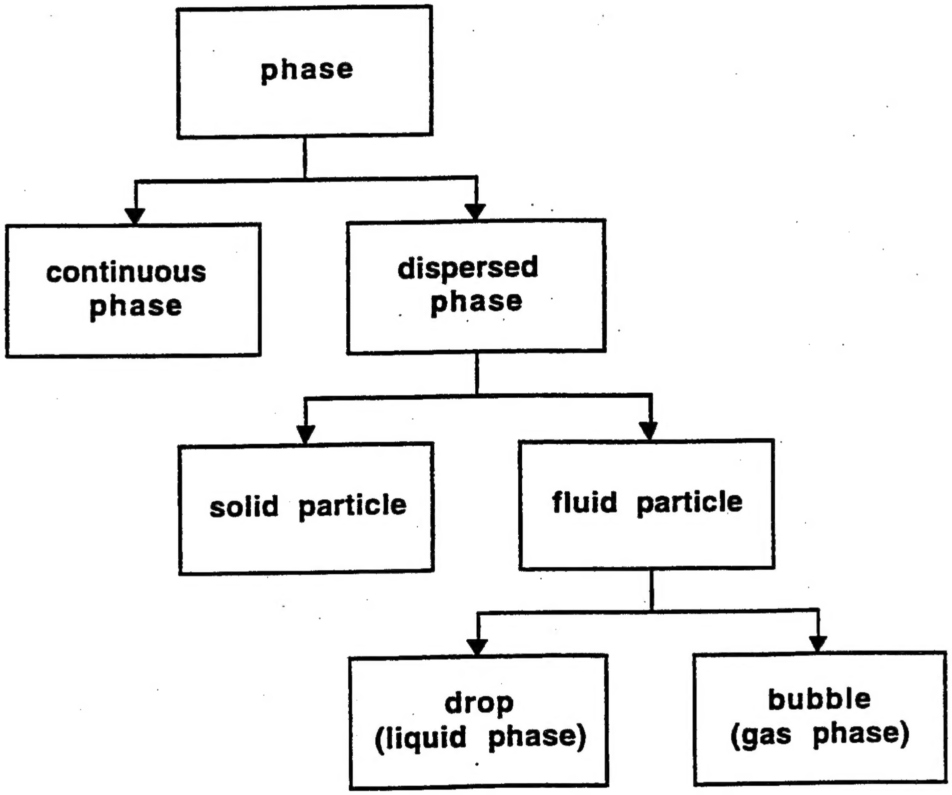

Figure 1. Classification of phase.

THEORETICAL BASIS

The theoretical basis of this study will be:

- conservation of mass
- conservation of momentum (Newton's second law)
- conservation of energy

These three principles are the theoretical basis for heat transfer and hydrodynamics, or general fluid mechanics. Their relationship with this study on bubbles is shown in Figure 2.

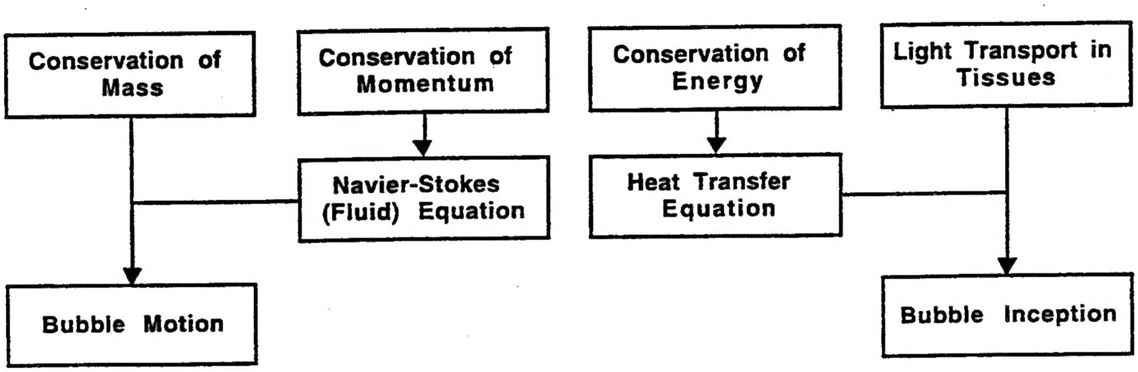

Figure 2. Theoretical basis of this study.

BASIC HEAT TRANSFER

If we select an infinitesimal element and apply the principle of conservation of energy, which is heat in this context, we obtain the general heat conduction equation:

$$\rho c \frac{\partial T}{\partial t} = \nabla \bullet (\kappa \nabla T) + Q, \tag{1}$$

where

- ρ: density [kilogram (kg)/meter (m)^3]
- c: mass specific heat [Joules (J)/(kg °K)]
- T: temperature [°K]
- t: time [seconds (s)]
- κ: thermal conductivity [watts (W)/(m °K)], meaning the heat flow per unit time per unit length per unit temperature gradient
- Q: heat source [W/m^3], heat generation per unit time per unit volume

In Equation 1, the left-hand side is the net increase of heat/energy per unit time per unit volume. The first term on the right-hand side is the net heat/energy flow into the infinitesimal element per unit time per unit volume, and the second term is the heat generation per unit time per unit volume due to the heat source.

When κ is a constant, the heat conduction equation (Equation 1) becomes,

$$\rho c \frac{\partial T}{\partial t} = \kappa \nabla^2 T + Q. \tag{2}$$

Thermal diffusivity is defined as the thermal conductivity (κ) divided by the volume specific heat (ρc), i.e.,

$$\alpha = \frac{\kappa}{\rho c}, \tag{3}$$

therefore,

α: thermal diffusivity [m^2/s]. Using Equation 3, Equation 2 may be reformulated into:

$$\frac{\partial T}{\partial t} = \alpha \nabla^2 T + \frac{Q}{\rho c}. \tag{4}$$

BASIC HYDRODYNAMICS

If we select an infinitesimal element and apply Newton's second law, we can obtain the Navier-Stokes equation for an incompressible fluid:

$$\rho \frac{d\mathbf{u}}{dt} = \rho \mathbf{g} - \nabla p + \mu \nabla^2 \mathbf{u}, \tag{5}$$

where

ρ: density [kg/m^3]
u: velocity vector [m/s]
t: time [s]
g: gravitational acceleration vector [9.8 m/s^2]
p: pressure [pascal or Newtons (N)/m^2]
μ: viscosity [pascal s], defined as the shear stress divided by the shear rate (i.e., velocity gradient)

In Equation 5, the left-hand side is the mass per unit volume multiplied by the acceleration of the infinitesimal element. The total derivative can be expanded to:

$$\frac{d\mathbf{u}}{dt} = \frac{\partial \mathbf{u}}{\partial t} + \mathbf{u} \bullet \nabla \mathbf{u}, \tag{6}$$

in which the first term, called the local derivative, represents changes at a fixed point in the fluid and the second term, the convective term, accounts for changes following the motion of the fluid.

The first term on the right-hand side of Equation 5 is the gravity force, the second term is the pressure gradient generated force, and the third term is the viscosity generated force acting on the infinitesimal element. If the gravity force is merged into the pressure, and the viscosity is ignored, then Equation 5 becomes:

$$\rho \frac{d\mathbf{u}}{dt} = -\nabla p, \tag{7}$$

which is considered an expression of conservation of momentum.

The conservation of mass leads to:

$$\frac{\partial \rho}{\partial t} + \nabla \bullet (\rho \mathbf{u}) = 0, \tag{8}$$

where the first term is the local mass increase in an infinitesimal element per unit time per unit volume, and the second term is the net mass transport out of the element per unit time per unit volume. Note that $\rho\mathbf{u}$ is the mass flow rate (i.e., mass flow per unit time per unit area in the units of $kg/(m^2\ s)$.

The conservation of energy leads to:

$$\rho\frac{d}{dt}\left[E+\frac{1}{2}\mathbf{u}\bullet\mathbf{u}\right]=-\nabla\bullet(p\mathbf{u}), \tag{9}$$

where E is the internal energy per unit mass, and 1/2 $\mathbf{u}\bullet\mathbf{u}$ is the kinetic energy per unit mass. Note that $p\mathbf{u}$ is the work done per unit time per unit area in the units of $J/(m^2 \bullet s)$.

STUDIES OF UNDERWATER EXPLOSIONS

The research results of underwater explosions in the 1940s may be borrowed to benefit our research.[2] The underwater explosion is initiated with, say, 150 kg TNT. The temperature near the explosion can be as high as 3,000° C, and the pressure can reach 50,000 bars.

Detonation Wave

With the high explosives such as TNT, the chemical transformation occurs so rapidly that it can keep up with the physical disturbance resulting from the reaction. A reaction occurring in this way develops a very narrow boundary between material in its initial condition and the products at high temperatures and pressure. This clearly defined, rapidly advancing discontinuity is know as a "detonation wave" and travels with a velocity of several thousand meters per second.

Burning

On the other hand, the chemical reaction may take place more slowly and be unable to keep up with the advancing physical disturbance of pressure and particle motion that it causes. The final reaction state is then reached more gradually and there is not a well-defined boundary. This more gradual process is called "burning," although the rate at which it occurs may still be high. Propellants such as gunpowder, which burn with a gradual building up to the final state, are used to drive a shell, rocket, airplane, etc.

Shock Wave

Once the detonation wave is initiated, the disturbance is propagated radially outward as a wave of compression in the water, and the steep fronted wave is described as the "shock wave." As compared to waves of infinitesimal amplitude, this shock wave has the following characteristics:

(1) The velocity of propagation near the charge is several times the limiting value of about 1,667 m/s. This value is approached quite rapidly as the wave advances outward, and the pressure falls to "acoustic" values.

(2) The pressure level in the spherical wave falls off more rapidly with distance than the inverse first power law predicted for small amplitudes, but eventually approaches the behavior in the limit of large distances.

(3) The profile of the wave broadens gradually as the wave spreads out. This spreading effect is most marked in the region of high pressure near the charge.

Bubbles

Once the shock wave is emitted, a bubble will form around the explosion site. Several steps include:

(1) Bubble expansion. The bubble expands faster than expected as a result of the afterflow of the shock wave. Bubble pressure decreases, but expansion continues for a relatively long time because of the inertia of the outward flowing water.

(2) Maximum bubble expansion. Gas pressure falls below the equilibrium pressure determined by the atmospheric plus hydrostatic pressure. The expansion stops.

(3) Bubble contraction. The bubble contracts at an increasing rate, compresses gas, and increases the gas pressure.

(4) Minimum bubble contraction. The gas compressibility acts as a powerful check to reverse the motion abruptly.

(5) Bubble oscillation. Repeat steps (2) through (4). The oscillation period is:

$$T \propto \frac{E^{1/3}}{p^{5/6}} \qquad (10)$$

where E is the internal energy of the gas, and p is the hydrostatic pressure of the water valid in the absence of disturbing effects due to boundaries.

(6) Bubble buoyancy. The bubble eventually rises to the surface due to the buoyancy.

If the water is considered incompressible, the pressure in the water should depend on the square of the rate of bubble expansion or contraction, and the rate reaches maximum when the bubble size reaches minimum. The peak pressure of the first bubble pulse is no more than 10-20% of that of the initial shock wave, but the duration is much greater. The areas under the pressure-time curves are comparable. The relation between shock wave and bubble pulse pressures and durations is shown in the sketch of Figure 3.

Bubble Repulsion and Attraction

The bubble was found to experience a net repulsive force away from a free surface and will be attracted toward a rigid boundary.

Principle of Similarity

If the linear size of the charge is changed by a factor k (the weight changed by a factor k^3), the pressure conditions will be unchanged if new distance and time scale k times as large as the original ones are used.

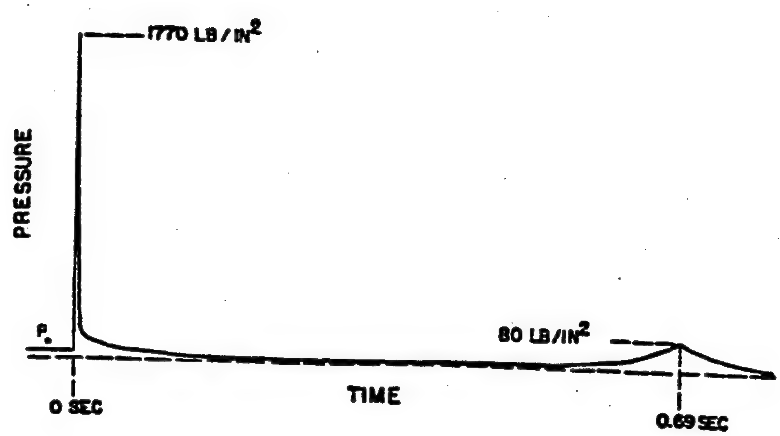

Figure 3. Pressure-time curve of detonation. Pressure 60 feet (ft) from a 300 pound (lb) TNT charge fired 50 ft below the surface. One lb/inch $(in)^2$ is approximately 0.07 bars.

EFFECT OF LONG-PULSE LASERS

Asshauer et al. have recently reported the observation of acoustic transients in pulsed holmium laser ablation underwater.[3] In their experiments, 2.2-micrometer (μm) chromium:thulium:holmium:yttrium-aluminum-garnet (Cr:Tm:Ho:YAG) laser pulses were delivered via a fiber underwater. The pulse durations are varied from 130-230 microseconds (μs) and pulse energies from 20-800 millijoules (mJ).

The key result of their experiment is shown in Figure 4. The 180 bar pressure peak in Figure 4 was reached when the bubble size was minimal. Assuming the 1/r dependence of pressure, where r is the radial distance from the center of the shock wave, they computed that the pressure at 0.5 millimeters (mm) from the center is more than 1,000 bars. However, only a pressure increase on the order of 1 bar was observed during the laser pulse after 75 μs.

The stress relaxation time of the laser heated area is about (600 μm)/(1.5 mm/μs) = 0.4 μs. The laser pulse (130-230 μs) was not short enough to build up a shock wave. The pressure keeps "leaking out" as the later part of the pulse comes in. Therefore, the ablation process is a "burning" process as defined in the last section.

Asshauer et al.[3] have also found that bubbles will be attracted toward a rigid boundary as stated by Cole.[2] It is nice to see that the laws of physics have not changed after half a century.

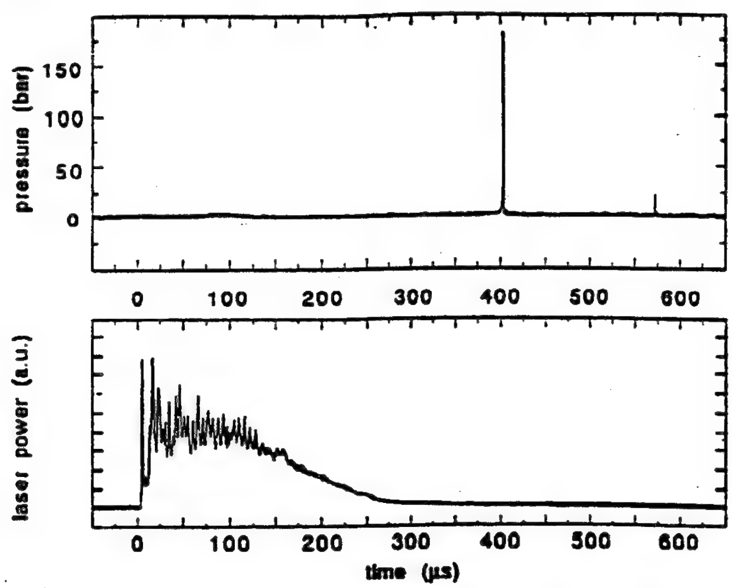

Figure 4. Pressure-time curve of bubble collapse and profile and laser pulse. Upper: Pressure amplitude measured by a Polyvinylidene Fluoride (PVDF) needle probe hydrophone at 3 mm distance from the bubble collapse center. Fiber core diameter 600 μm.
Lower: Temporal pulse shape of the Cr:Tm:Ho:YAG laser for 424 mJ energy, 180μs full-width-half maximum (FWHM) pulse duration.

EFFECT OF SHORT-PULSE LASERS

The problem we are interested in involves short-pulse lasers. It is important to keep the scales of all the dimensions and processes in mind,[4] i.e.,

1.0-µm diameter of melanin granule, d
100-picosecond (ps) laser pulsewidth
~700-ps stress relaxation time
~2-µs thermal relaxation time

The stress relaxation time of the granule is computed by:

$$d/v = (1.0\ \mu m)/(1.5\ mm/\mu s) \approx 700\ ps,$$

where v is the velocity of stress wave. The thermal relaxation time of the granule is computed by:

$$d^2/(4\,\alpha) = (1.0\ \mu m)^2 / (4\times1.4\times10^{-3}\ cm^2/s) \approx 2\ \mu s.$$

Because the laser pulse is much shorter than the thermal relaxation time, the optical propagation and the thermal propagation can be considered separately.

If the fluence of the laser beam is F [J/centimeters $(cm)^2$], and the absorption coefficient of the melanin granule is μ_a [cm^{-1}], then the peak energy density will be Q' [J/cm^3]:

$$Q' = \mu_a F, \tag{11}$$

where μ_a is wavelength dependent:

$$\mu_a = 6.6\times10^{11} / \lambda^{3.3}, \tag{12}$$

where λ is in the units of nanometers (nm) and μ_a is in the units of cm^{-1}.[4]

When the laser pulsewidth is comparable to or shorter than the stress relaxation time, pressure is able to build up to generate a shock wave. Therefore, with a short-pulse laser, the laser energy is dumped into the medium fast enough to keep up with the physical disturbance. A shock wave can be generated followed by subsequent bubble pulses caused by bubble collapses. On the other hand, the long-pulse lasers cannot keep up with the physical disturbance. As a result, only a "burning" process occurs, and no initial shock wave will be generated although bubble pulses will still be generated.

Because the initial shock wave is 5-10 times stronger than the first bubble pulse according to the studies of underwater explosion,[2] the minimal energy density required to cause MVL (see Figure 5) will be reduced by a factor of 5-10 if the initial shock wave is

generated. This explains why there is a 5-10 fold drop in the minimal energy density required to cause MVL when the pulsewidth of the laser is shortened from the nanosecond range to the subnanosecond range, where the experimental results of many other researchers were summarized by Jacques et al.[4]

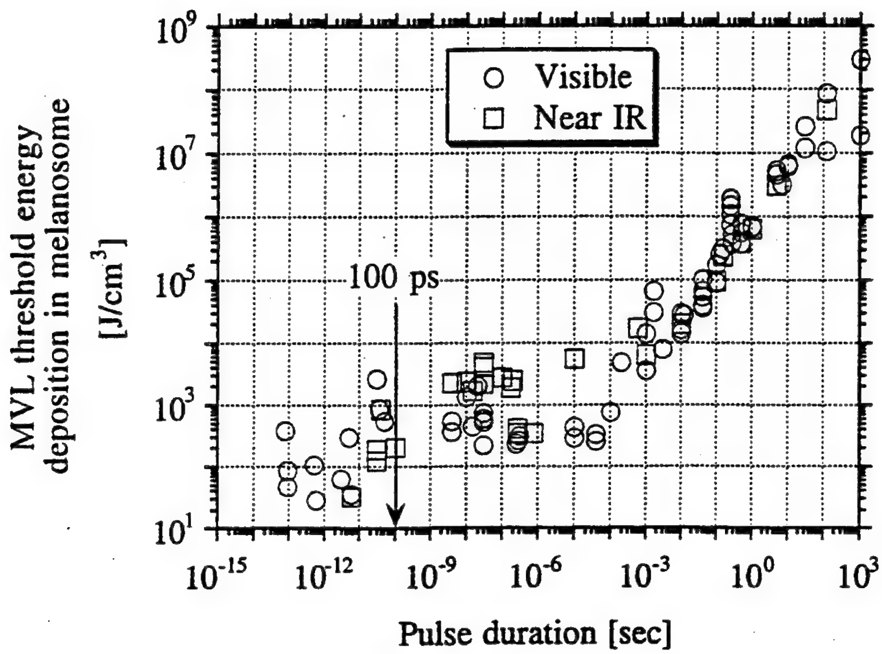

Figure 5. Minimal energy density causing retinal MVL.

MOTION OF UNDERWATER EXPLOSION BUBBLES

This section will review the early studies of motion of underwater explosion bubbles,[2] from which we can learn the general picture of bubble motion. After emission of the shock wave, the gaseous products of an explosion continue to expand outward at a gradually decreasing rate. As a result there are considerable radial displacements of the water, but the changes in velocity take place at a much slower rate than in the initial phases of the motion immediately following detonation. The pressures in the surrounding liquid are therefore much smaller and the whole character of the motion changes. Although the same basic hydrodynamic equations apply as in the case of the shock wave, and exact solutions would be at least as difficult to obtain, the qualitative differences in the later motion make more appropriate somewhat different approximations. In order to see the reasons for these and their limitations, it is helpful to examine briefly some

experimental studies of the motion before considering the various theoretical developments.

A series of frames from a motion picture record of bubble motion were taken; the charge used was 0.55 lb of tetryl detonated 300 ft below the surface of the water. The bubble radius is plotted as a function of time in Figure 6. The time intervals between these frames are all nearly equal, and it is evident that an initial rapid expansion of the spherical bubble is gradually brought to a stop after 14 milliseconds (ms). The bubble then contracts at an increasingly rapid rate until it reaches a minimum 28 ms later, and after an abrupt reversal again expands. Throughout the expanded phase of the bubble's motion there is very little vertical migration, but near the minimum radius an appreciable upward displacement occurs. The reversal of the bubble motion at the minimum occurs so abruptly as to be virtually discontinuous on a time scale suitable for the rest of the motion; this characteristic is shown clearly in Figure 6. A further qualitative feature of significance is the fact that the bubble retains its identity at the minimum despite the large radial accelerations and appreciable vertical motion, and remains fairly symmetrical. The motion is, therefore, a reasonably stable one in fact. A further evidence of overall stability is the continued oscillations of the bubble (if the charge is fired sufficiently deep to permit them to occur before the bubble rises to the surface): three or four complete cycles are readily observed and at least ten such cycles have been shown to exist for very deep charges.

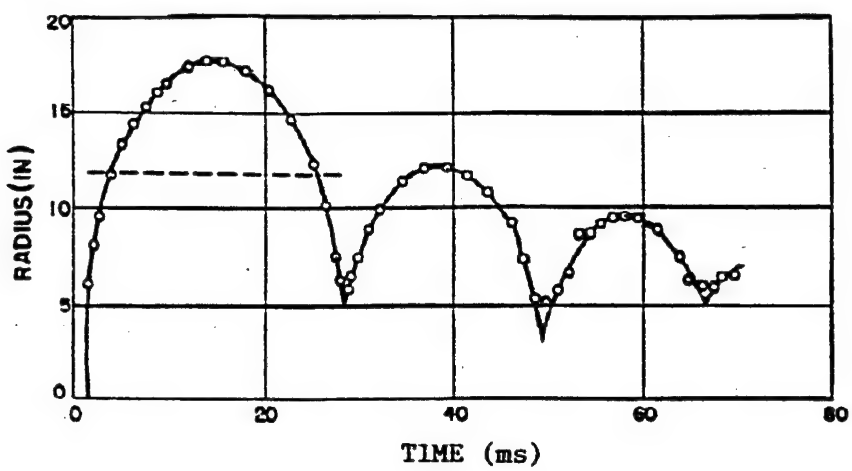

Figure 6. Radius-time curve of bubble. The data were for a 0.55 lb tetryl charge 300 ft below the surface.

The maximum velocity of the bubble surface as the bubble approaches minimum radius is about 200 ft/s in the example and over most of the motion is very much less. The maximum radius of 1.48 ft corresponds to an internal gas pressure very much less than hydrostatic (roughly one-fifth), as the equilibrium radius for this size charge is readily estimated to be 1.0 ft. This radius, for which the gas is at the hydrostatic pressure of the water, is indicated by the dashed line in Figure 6, and it is evident that the pressure is less than this over some 80% of the first cycle. The length and time scales will of course change with the size of charge and the depth at which it is fired, being larger for larger

charges and shallower depths. In general, however, it is true that the radial velocities will be of the same order of magnitude, and that over most of the cycle the pressures are much smaller than hydrostatic.

These conclusions about the bubble motion are the basis of all the bubble theories which lead to general numerical predictions of bubble radius, migration, and period. It is a common characteristic of such theories that changes in density of the water surrounding the bubble are neglected (the noncompressive approximation) and it is further assumed that the bubble retains a spherical form throughout the motion. From what has been said, it is evident that both these assumptions are at least plausible as far as the expanded phase of the motion is concerned. They must, however, be increasingly poor as the bubble approaches its minimum radius for which very much larger pressures and acceleration are involved. At this radius, for example, pressure waves (the secondary or bubble pulses) are emitted, which an incompressive theory can describe only as a disturbance appearing simultaneously at all points in the liquid.

From the foregoing considerations, it is to be expected that the theories based on noncompressive flow will be most successful in accounting for the general properties of the motion in its expanded phases, and in predicting properties, such as the period, primarily thus determined. The vertical displacement of the bubble at its minimum and the characteristics of the pressure wave emitted at that time are, however, more seriously affected by the approximations. In addition to the common assumptions just described all the theories involve other approximations, and the degree of refinement of the various treatments is largely a question of the extent to which these further approximations and idealizations are removed.

THEORY OF BUBBLE MOTION - NONCOMPRESSIVE SURROUNDING MEDIUM

This section will discuss a simple theory of bubble motion -- noncompressive radial motion neglecting gravity.[1,2] This theory was originally developed for underwater explosions, but should apply to laser-generated bubbles as well. For the convenience of reference, symbols and their units are listed below.

t: time [s]
r_0: equilibrium density [kg/m^3]
P_0: equilibrium pressure [Pascal]
a_0: initial radius of bubble motion [m]
a_m: maximum radius of bubble motion [m]
a: radius of bubble motion [m]
T: oscillation period of bubble motion [s]
Y: total energy of bubble [J]

The simplest approximation to the true motion of the gas bubble is the one in which it is assumed that the motion of the surrounding water is entirely radial and there is no vertical migration. In this approximation, which has been discussed by a number of authors, the hydrostatic buoyancy resulting from differences in hydrostatic pressure at different depths is neglected. It is thus assumed that at an infinite distance from the bubble in any direction the pressure has the same value as the initial hydrostatic pressure P_0 at the depth of the charge or the absorber of laser light (atmospheric plus the added pressure of the water column). For a given depth of charge (or absorber), the differences in pressure at the surface or near the bubble will clearly be greater the larger the charge and bubble resulting from its deformation. The neglect of differences in hydrostatic pressure should thus be more serious for large charges and small depths. In our application, the laser-induced bubbles are expected to be so small that the differences in hydrostatic pressure are negligible.

If radial flow is assumed, the equations of continuity and motion for the water are (see Equations 7 and 8):

$$\frac{\partial \rho}{\partial t}+u\frac{\partial \rho}{\partial r}+\rho\frac{\partial u}{\partial r}+\frac{2\rho u}{r}=0, \qquad (13a)$$

$$\rho\frac{\partial u}{\partial t}+\rho u\frac{\partial u}{\partial r}+\frac{\partial P}{\partial r}=0. \qquad (13b)$$

where u is the radial component of the velocity **u**. Because the compressibility of water is only about 5×10^{-5} bar^{-1}, for pressure changes of the order 15 lb/in^2 or 1 bar, such as prevail over most of the bubble motion, the corresponding changes in density are of the order $10^{-4}\ \rho_0$ where ρ_0 is the equilibrium density. Under these conditions, the derivatives of density ρ are easily seen to be negligible in Equation 13a, which then becomes

$$\frac{\partial u}{\partial r}=-\frac{2u}{r}.$$

Integrating this equation, we have:

$$u(r,t)=\frac{u_1(t)}{r^2}, \qquad (14)$$

where the constant of integration $u_1(t)$ is the velocity for r = 1 and may depend on time. The radial velocity in noncompressive flow thus falls off as the inverse square of the distance from the origin, as is, of course, evident from elementary principles. With this result, the Equation (13a), becomes:

$$\frac{1}{r^2}\rho_0\frac{du_1}{dt}+\frac{1}{2}\rho_0\frac{\partial u^2}{\partial r}+\frac{\partial P}{\partial r}=0. \qquad (15)$$

Integrating from the surface of the gas sphere, for which $r = a$, $u_a = da/dt = u_1/a^2$, $P = P_a$, to infinite distance where $P = P_0$ and $u = 0$, gives:

$$\frac{\rho_0}{a}\frac{d}{dt}\left(a^2\frac{da}{dt}\right)-\frac{1}{2}\rho_0\left(\frac{da}{dt}\right)^2-\left(P_a-P_0\right)=0.$$

Integrating with respect to time leads to the result:

$$\frac{1}{2}\rho_0\, a^3\left(\frac{da}{dt}\right)^2+\frac{1}{3}P_0\, a^3-\int_0^t P_a\, a^2 da = C', \tag{16}$$

where C' is a constant of integration. Except for a factor 4π, the integral over *a* is easily seen to represent the work done by the pressure P_a in expanding the sphere to its radius a(t), as the element of volume is $dV = 4\pi a^2 da$, and the integral must therefore equal the decrease in internal energy of the gas to E(a) from its initial value. Absorbing this initial value into a new constant of integration Y gives after rearrangement:

$$\frac{3}{2}\left(\frac{4\pi}{3}\rho_0 a^3\right)\left(\frac{da}{dt}\right)^2+\frac{4\pi}{3}P_0 a^3+E(a)=Y. \tag{17}$$

Written in this form, it is easily seen that the first time integral of the equation of motion is merely the expression of conservation of energy, as the first term is readily shown to be the kinetic energy of the radial flow outside the boundary, and the second term is the work done against hydrostatic pressure.

If the products of explosion or the laser-induced vapor behave as ideal gases with a constant ratio of specific heats g and are further assumed to undergo adiabatic changes, the pressure-volume relation is $P(V/W)^{\gamma} = k$, where W is the mass of explosive products or the laser-induced vapor in grams and k is a constant. The internal energy E(a) is then given by:

$$E(a)=\int_{V(a)}^{\infty} PdV=\frac{P_a V(a)}{\gamma\text{ -1}}=\frac{kW}{\gamma\text{ -1}}\left(\frac{W}{V(a)}\right)^{\gamma-1}.$$

From the last expression, it is evident that E(a) decreases rapidly with increasing volume (proportional to a^3), and at sufficiently expanded stages of the motion represents a negligible fraction of the initial energy of the products. The values of radius *a* and corresponding pressure P_a for which E(a) has a given value can be estimated from a knowledge of the adiabatic law for the products and the initial energy. For TNT, the calculations of Jones (described in section 3.5 of Cole[2]) give the adiabatic relation, valid for $P < 4{,}500$ lb/in.^{2}

$$P\left(\frac{V}{W}\right)^{1.25} = 7.8,$$

where P is in kilobars, W is in grams, and V is in cm^3. The total energy released by 1 gram of TNT is about 1,060 cal/gm (= 4.44×10^{10} ergs/gm) of which approximately half is emitted in the shock wave.

The fraction F of the remaining energy Y which is present as internal energy at any state of expansion is:

$$F = \frac{E(a)}{Y} = 0.166\ P_a^{1/5} = 0.42\left(\frac{W}{a^3}\right)^{1/4},$$

where P is in lb/in^2, W is in lb, a in ft., and Y is taken to be 440 calories (cal)/gram (gm). This fraction is less than 25% for P < 7.6 lb/in^2. For a 300-lb charge the corresponding radius is 13.5 ft, rather less than the maximum radius of about 20 ft for a charge detonated 50 ft below the surface. The curve of bubble expansion has the same qualitative manner of variation with time as shown in Figure 6, which leads to the estimate that the internal energy of the products is less than 25% of the total for more than 70% of the entire cycle.

The fact that the internal energy is relatively unimportant over much of the expansion suggests, as a first approximation, neglecting it entirely. If this is done, it will be seen that the gas sphere must have a maximum radius when da/dt = 0. Calling this value a_m, we have from Equation 17:

$$Y = \frac{4\pi}{3} P_0\, a_m^{\ 3}. \tag{18}$$

This relation thus furnishes an experimental method for determining, to a rather good approximation, the total energy Y associated with the radial flow of water in terms of the maximum radius a_m of the bubble and the hydrostatic pressure P_0 at the depth of the explosion.

Neglecting the internal energy in Equation 17 makes possible separation of the variables, and using Equation 18 to eliminate Y gives the result:

$$t = \sqrt{\frac{3\rho_0}{2P_0}} \int_{a_0}^{a} \frac{da}{\sqrt{\left(\frac{a_m}{a}\right)^3 - 1}}, \tag{19}$$

where a_0 is the initial radius of the gas sphere at time t = 0. The integral is not expressible in terms of elementary functions, but can be transformed to give a sum of incomplete b-functions $B_x(p, q)$, defined by:

$$B_x(p,q) = \int_0^x x^{p-1}(1-x)^{q-1}dx,$$

the necessary substitution being $x = (a_m/a)^3$. Values of this function have been tabulated for discrete values of p, but unfortunately the values $p = 5/6$, $q = 1/2$ required here are apparently not included. In general, the solution must therefore be obtained by numerical methods, and some of these results are illustrated later. In the particular case $x = 1$, corresponding to $a = a_m$, the solution is known in terms of the factorial or G-function: $B_1(5/6, 1/2) = 2.24$. These limits $a = 0$, a_m correspond to the time required for expansion from zero to maximum radius. The initial radius a_0 is small compared to a_m and hence this time is approximately 1/2 the period of oscillation T. Substitution in Equation 19 gives the approximate result:

$$T = \frac{2}{3} a_m \sqrt{\frac{3\rho_0}{2P_0}} B_1(5/6, 1/2) = 1.83\, a_m \sqrt{\frac{\rho_0}{P_0}}. \qquad (20)$$

This equation can be used to compute the period of oscillation for the experiment presented in Figure 4. The maximum radius was measured to be 1.4 mm, and the period was measured to be 370 μs. Substituting $a_m = 0.0014$ m, $\rho_0 = 1000$ kg/m^3, and $P_0 = 10^5$ Pascal into Equation 20, we obtain T = 260 μs. The discrepancy was caused by at least two factors: (1) the bubble in the experiment was not circular; (2) the laser pulse was so long that the light energy was still being absorbed after the bubble started expansion.

This result can also be expressed in terms of the total energy Y by Equation 18, giving:

$$T = 1.14\sqrt{\rho_0}\, \frac{Y^{1/3}}{P_0^{5/6}}. \qquad (21)$$

This expression, which has been derived by a number of authors and is usually known as the Willis formula, shows that the "bubble period" varies as the cube root of the total energy or weight of a given explosive and, for a given weight, varies as the negative 5/6 power of the hydrostatic pressure. The particular constant multiplying the period formula depends, of course, on the limit of integration chosen for the initial radius. The functional dependence of the period on Y, P_0, ρ_0 must, however, be in the form of Equation 21 from dimensional considerations, if these variables are assumed to be the only ones affecting the motion. It is therefore reasonable to expect that this form should apply more generally than the approximations of the simplified model would permit. The experimental evidence does in fact demonstrate the validity of the formula over a wide range of depths provided the multiplying factor is suitably adjusted. However, this agreement is not found for charges fired near the surface or bottom, which is to be expected as a result of the

distortion of the mass flow of water by such boundaries. The modifications of the simple formula obtained by more refined analysis need to be considered.

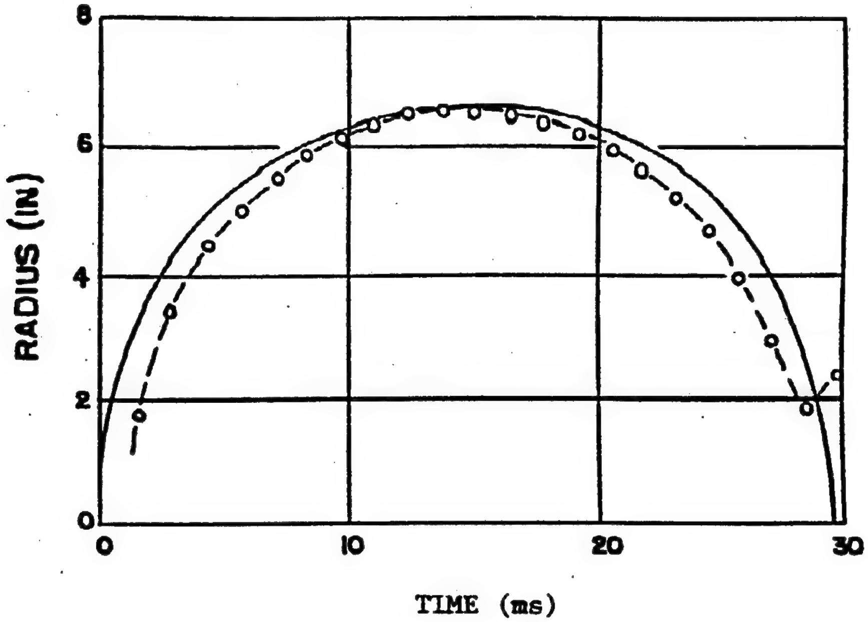

Figure 7. Verification of the computed radius-time curve. Measured and calculated radius of the gas sphere from a detonator one foot below the surface.

A comparison between experimental results and theoretical computations is shown in Figure 7. The experimental points are taken from high-speed motion picture of the bubble motion, and the solid curve is taken from theoretical calculations based on Equation 19, the value of a_m having been chosen to give agreement with the experimental observations. It is seen that the simple theory predicts a curve of the same general form but somewhat broader than that found experimentally. The most likely explanations of the difference appear to be either that optical distortions in the experimental arrangement caused errors or that the proximity of the free surface 12 inches above the charge and a steel plate beneath it had significant effects.

In summary, Equation 19 should be used to compute the radius-time curve of the bubble motion. The equilibrium density r_0 and the hydrostatic pressure P_0 are known. The minimum and maximum radii have to be provided to solve the equation. The maximum radius is related to the total internal energy of the bubble by Equation 18. Therefore, the maximum radius can be estimated if the total energy is known.

THEORY OF BUBBLE MOTION - COMPRESSIVE SURROUNDING MEDIUM

The approximate theory of bubble pulsation and migration on the simplifying assumption that the surrounding water was incompressible was developed in the last

section. Although most of the calculations of the motion suitable for comparison with experimental data have been made with these approximations, more exact formulations undertaken by Herring[5] and others are of interest in indicating the nature of the errors to be expected from the simpler calculations.

The equation of an inviscid fluid for spherical symmetry is Equation 13b, where u is the radial velocity and P the pressure at a point (r, t). Integrating Equation 13b from the bubble surface (r = a) to infinity gives,

$$a\frac{d^2a}{dt^2}+\frac{3}{2}\left(\frac{da}{dt}\right)^2-a\frac{da}{dt}\lambda(a)+\int_a^\infty r\frac{\partial\lambda}{\partial t}dr=-\int_a^\infty\frac{dP}{\rho}, \tag{22}$$

where the variable λ has been defined as the divergence of the velocity u, i.e., $\lambda = (1/r^2)\,\partial/\partial r\,(r^2u)$.

If we assume that the density is a known function of pressure P, neglecting irreversible processes induced by the preceding shock wave, the right side of Equation 22 is a known function of P(a), the pressure in the gas sphere. The departures from incompressible theory are represented by the terms in λ. It can be seen from Equation 14 that $\lambda = 0$ for an incompressible medium. The equation of continuity (Equation 13a) supplies a means for evaluation $\lambda(a)$ in terms of P(a), however, for we have from the theory of waves of finite amplitude[2] that,

$$\lambda(a)=[\mathrm{div}\,u]_{r=a}=\left[-\frac{1}{\rho}\frac{d\rho}{dt}\right]_{r=a}=\left[-\frac{1}{c^2\rho}\frac{dP}{dt}\right]_{r=a}, \tag{23}$$

where $c^2 = (dP/d\rho)_s$ is the velocity of sound. With this relation, Equation 22 becomes an ordinary differential equation for *a* in terms of P(a), except for the integral

$$\int_a^\infty r\frac{\partial\lambda}{\partial t}dr.$$

This term is the only one that can account for loss of energy by radiation of a pressure pulse, as the others are unaffected by a change in the sign of u(a) = da/dt. If the motion of the water is sufficiently small for acoustic theory to be applied, this integral would be given exactly by a simple analysis. For in the limit of small amplitudes, the velocity u, and hence its divergence λ, must satisfy the wave equation,

$$\Delta^2\lambda-\left(1/c_0{}^2\right)\partial^2\lambda/\partial t^2=0.$$

Hence for spherical symmetry, λ is of the form $(1/r)\,f(t-r/c_0)$. We therefore have,

$$r\partial\lambda / \partial t = -c_0 \partial / \partial r(r\lambda),$$

and the integral in question becomes,

$$\int_a^\infty r \frac{\partial \lambda}{\partial t} dr = -c_0 \int_a^\infty \frac{\partial}{\partial r}(r\lambda)\, dr = c_0 a\, \lambda(a). \tag{24}$$

In some cases, the amplitude of motion is sufficiently large that the acoustic theory is not valid, but Herring[5] has shown that the deviations from the acoustic result of Equation 24 are not large, being greatest at and near the stage of greatest contraction. This analysis, not shown here, shows that the most important correction term to be added to the right side of Equation 24 is,

$$-\frac{1}{c_0 a}\frac{d}{dt}\left[a^2\left(\frac{da}{dt}\right)^2\right].$$

Substituting in Equation 22, using Equation 23 for $\lambda(a)$, and rearranging gives,

$$a\frac{d^2a}{dt^2} + \frac{3}{2}\left(\frac{da}{dt}\right)^2 - \frac{1}{ac_0}\frac{d}{dt}\left[a^2\left(\frac{da}{dt}\right)^2\right] = \frac{a}{\rho c_0}\frac{dP_a}{dt}\left(1 - \frac{1}{c_0}\frac{da}{dt}\right) - \int_a^\infty \frac{dP}{\rho}. \tag{25}$$

The left side of this equation can be written as a derivative, and if density variations are neglected so that ρ can be replaced by ρ_0, the density at the center of the bubble, we can integrate over *a*. Taking the lower limit to be the maximum radius a_m for which $da/dt = 0$, we obtain:

$$a^2\left(\frac{da}{dt}\right)^2\left(1 - \frac{4}{3}\frac{1}{c_0}\frac{da}{dt}\right) = \int_{a_m}^{a}\left[\frac{P_a - P_0}{\rho_0} + \frac{a}{\rho_0 c_0}\frac{dP_a}{dt}\left(1 - \frac{1}{c_0}\frac{d\,a}{dt}\right)\right]2a^2 da. \tag{26}$$

In Equation 26, the terms in $1/c_0$ represent approximately the effect of compressibility, and if these terms are neglected Equation 26 reduces to Equation 17, which is the energy equation for an incompressible medium. The factor,

$$\left(1 - \frac{4}{3}\frac{1}{c_0}\frac{da}{dt}\right)$$

changes sign when the bubble passes its maximum radius, as da/dt becomes negative, and hence introduces an asymmetry in the radius-time curve. In underwater explosions, this is not particularly important as da/dt, the radial velocity, is very much less than the velocity of sound c_0 over nearly the entire pulsation. The term involving dP(a)/dt represents the acoustic radiation of energy.

Equation 26 in principle permits a solution for the radius-time curve and the corresponding pressure at the surface of the bubble. It seems quite certain for underwater explosions that the deviations from noncompressive theory will be insignificant over most of any one cycle, although the radiation term does lead to a large energy loss near the minimum.

BUBBLE INCEPTION

Bubble formation is an important and complicated step. The elementary concept of inception is the formation of cavities at the instant the local pressure drops to the vapor pressure of the liquid. However, the problem is not so simple. Although experiments show that inception to occur near the vapor pressure, there are deviations of various degrees with both water and other liquids that are not reconcilable with the vapor-pressure concept. We define the vapor pressure as the equilibrium pressure, at a specified temperature, of the liquid's vapor that is in contact with an existing free surface. If a cavity is to be created in a homogeneous liquid, the liquid must be ruptured, and the stress required to do this is not measured by the vapor pressure but is the tensile strength of the liquid at that temperature. The question naturally arises then as to the magnitudes of tensile strengths and the relation these have to experimental findings about inception.

For a homogeneous liquid, the forces tending to hold liquid "particles" together are external pressure and intermolecular cohesive forces. The latter are evidenced in several ways. For example, the latent heat of vaporization exceeds the work done by vapor expansion against external pressures. Also, there are the properties of adhesion (wetting) and surface tension which liquids display. It is because of the intermolecular forces that liquids should be expected to support tension. The measurements of water have shown different values, ranging from 13 atmospheres (atm) to 157 atm, of tensile strength. The variation may have been caused by the container, the purity of the water, etc.

In the theory of liquids the existence of minute voids or "holes" is postulated. The liquid state is considered to be pseudo-crystalline with a large number of vacant sides. Fisher[6], Frenkel[7], and Furth[8] advanced theories to predict such "holes" in statistical equilibrium throughout the liquid as a result of random thermal fluctuations. Fisher[6] and Doring[9] estimated the rate of spontaneous formation per unit volume of liquid. The theories agree in predicting holes in statistical equilibrium having radii of the order of 10^{-8} cm. They also predict that for these holes to be centers for rupture (i.e., to expand unstably) tensions ranging from 4,000 to 10,000 atm would be required. However, this estimate differs by orders of magnitude from the experimental evidence previously reviewed. Finally, it can be shown that the probability, or rate, of spontaneous formation of holes in a given volume is negligible unless the liquid temperature is near its critical point. Thus, even at the extreme tensions indicated, the probability of rupture occurring within a reasonable length of time is negligible. It appears very doubtful that "holes" of this origin are of any consequence in determining observed tensile strengths or cavitation

or boiling pressures. Only if some mechanism allows growth and stabilization of these holes into permanent "nuclei" can they be important.

Turning attention to contamination, we note first that not all foreign materials added to a liquid will affect the cavitation process; unless it affects the formation, growth, or collapse of the cavities, the impurity will have little effect on cavitation. To make any significant change in the growth or collapse of existing cavities, the impurity must change appreciably such physical properties as viscosity, density, surface tension, thermal properties, etc. To do this it usually must be present in such large amounts that it will become a component of the system rather than an impurity. Thus attention will be focused upon the impurities that affect the formation of cavities by providing "weak spots."

Considerable information is available about the type of impurities that do not affect the tensile strength of a liquid. For example, the addition of a miscible liquid has little effect. In such a case, it would be expected that the minimum tensile strength would approximate that of the weaker of the two liquids, but since in any case this is several orders of magnitude greater than the maximum tension involved in liquid flow processes, it is not of importance. Likewise, dissolved solids produce little, if any, decrease in the effective tensile strength of the solvent.

The effects of nonmiscible and nonsoluble substances appear to be closely related in that a factor of major importance is the degree of wettability (i.e., the strength of the bond at the interface between the liquid and the solid, or between the two dissimilar liquids). Measurements of the contact angle between liquids and solids indicate that no liquid wets any solid perfectly and that all liquids wet all solids to some measurable extent. When the degree of wetting is low (hydrophobic) weak spots in the bond are apparently present, for cavities appear to form fairly readily on the solid surface. For example, in heating water in a metal container, vapor bubbles appear first on the surface of the metal even when the temperature of the metal is the same as that of the liquid.

Surface-tension forces always work in one direction (i.e., to close a cavity that is opened in a liquid). Since for a given liquid the tension is constant irrespective of the size of the cavity, it is much more significant in the case of small cavities than for large ones. Its most important effect is to decrease the rate of growth of the nuclei into finite cavities. Thus it is conceivable that in a flow system with a short negative-pressure zone a liquid with high surface-tension forces would develop no cavitation, whereas a liquid with low surface-tension forces and the same system of nuclei would cavitate. The action of surface tension in extremely small cavities is not quite clear. The basis of surface tension is molecular attraction, and when the surface of a nucleus becomes so small that it can contain only a limited number of molecules, then the surface-tension forces can no longer be considered as uniform and continuous. However, the nuclei responsible for normal cavitation have initial sizes that are probably at least one or two orders of magnitude greater than those for which the action of surface tension is questionable.

I am searching more data about the properties of melanin granules so that we can relate the above general information to our specific application.

SUMMARY

Conclusions or hypotheses will be summarized here.

Initial Shock Wave Induced by Subnanosecond Laser Pulses

When a subnanosecond laser beam is absorbed by a melanin granule buried underwater, the absorption of laser energy will cause a shock wave followed by bubble pulses of decreasing intensities. The initial shock wave will determine the threshold energy density required to cause MVL because the subsequent bubble pulses will be much weaker than the initial shock wave. The initial shock wave is 5-10 times stronger than the first bubble pulse. On the other hand, nanosecond or longer laser pulses are too long for the laser energy to build up the initial shock wave. This hypothesis seems to agree well with the experimental results that showed a 5-10 fold drop in the threshold energy density required to cause MVL when the pulsewidth of the laser is shortened from the nanosecond range to the subnanosecond range. However, a direct observation of the initial shock wave and the subsequent bubble pulses will be desirable to corroborate the theory.

Bubble Motion

A simple theory is presented in this report to compute the radius-time curve of the bubbles. The total energy of the bubble, among the hydrostatic pressure and the equilibrium density, is required to solve the equation numerically. It will be critical to estimate the total energy. It is difficult to estimate the total energy based on theory alone. Some experimental data will be needed for this estimation.

REFERENCES

1. Knapp, R.T., Daily, J.W., and Hammitt, F.G. *Cavitation.* New York: McGraw-Hill Book Co., 1970.

2. Cole, R.H. *Underwater Explosions.* Princeton University Press, 1948.

3. Asshauer, T., Rink, K., Delacretaz, G., Salathe, R.P., Gerber, B., Frenz, M., Pratisto, H., Ith, M., Romano, V., and Weber, H.P. Acoustic transient generation in pulsed holmium laser ablation underwater. *Proc SPIE, 2134,* 423-433 (1994).

4. Jacques, S.L., Oraevsky, A.A., Thompson, R., and Gerstman, B.S. A working theory and experiments on photoacoustic disruption of melanosomes to explain the threshold minimal visible retinal lesions for subnanosecond laser pulses. *Proc SPIE, 2134,* 54-65 (1994).

5. Herring, C. Theory of the pulsations of the gas bubble produced by an underwater explosion. *NRDC Division 6 Report C4-sr20* (1941).

6. Fisher, J.C. The fracture of liquids. *Sci Monthly, 68,* 415 (1949). [Also published in *J Appl Phys, 19,* 1062 (1948).]

7. Frenkel, J. *Kinetic Theory of Liquids*. Oxford: Clarendon Press, 1946.

8. Furth, R. On the theory of holes in liquid. *Proc Phys Soc (Lond), 52,* 768 (1940).

9. Doring, W. Die uberhitzungrenze und Zerreissfestigkeit von flussigkeiten. *Z Physik Chem, B38,* 292 (1939). [Also published in *Z Physik Chem, B36,* 371 (1937).]